Unsteady Entrance Flows in Elastic Tubes with Application to the Vascular System

NORMAN R. KUCHAR*
General Electric Company, Philadelphia, Pa.

AND

SIMON OSTRACH†
Case Western Reserve University, Cleveland, Ohio

Flow development effects in the large arteries are investigated analytically using a mathematical model of pulsatile, viscous flow in a semi-infinite, thick-walled elastic tube. A coupled set of differential equations and boundary conditions for the fluid and tube motions, containing approximations valid for the large arteries, is solved using Fourier series and Laplace transform techniques. Results include fluid velocity and pressure distributions and tube wall displacements and stresses. It is found that flow development depends primarily on the Reynolds number and the unsteadiness parameter with wall elasticity of secondary importance. The development length is comparable to the lengths of many arteries, and within the development region wall shear stresses are high. Thus, flow development effects can be important in the large arteries.

Nomenclature

a = unstressed internal tube radius
c = complex propagation velocity
c_x = friction coefficient of axial tethering
E = Young's modulus
F,f = fluid velocity at tube entrance
g = pressure at tube entrance
h = p-g
i = $(-1)^{1/2}$
k_x = spring coefficient of axial tethering
m_x = mass coefficient of axial tethering
n = harmonic number
N = highest harmonic in finite Fourier polynomial
P,p = pressure
p_e = perivascular pressure
R,r = radial coordinate
Re = Reynolds number, F_0a/ν
s = Laplace parameter
T,t = time
U,u = axial fluid velocity
V,v = radial fluid velocity
X,x = axial coordinate
α = unsteadiness parameter, $a(\omega/\nu)^{1/2}$
β = dimensionless external tube radius
γ = elasticity constant [Eq. (9)]
ϵ = elasticity parameter [Eq. (19)]
H,η = radial wall displacement
Θ = azimuthal coordinate
λ = eigenvalue
μ = Lamé coefficient
ν = kinematic viscosity
Ξ,ξ = axial wall displacement
ρ = fluid density
σ = Poisson ratio
$\tau_{\theta\theta},\tau_{rx}$ = hoop and shear stress in the tube wall
ω = angular frequency
$(^-)$ = Laplace transformed variable
$[\ ]$ = matrix
$[\ ]^{-1}$ = inverse matrix

Presented as Paper 70-786 at the AIAA 3rd Fluid and Plasma Dynamics Conference, Los Angeles, Calif., June 29–July 1, 1970; received July 17, 1970; revision received April 20, 1971. This research was supported by NASA under Grant NGR-36-003-088.

* Group Leader—Biofluid Mechanics, Environmental Sciences Laboratory.

† Professor of Engineering. Associate Fellow AIAA.

I. Introduction

MOST theoretical investigations of blood flow in the large vessels have concentrated on the fully developed region, that is, that portion of the flowfield located far enough from the vessel ends or other geometrical discontinuities so that end effects are negligible.[1,2] Much has been learned about the nature of pulsatile flow and wave propagation in the arteries. However, these analyses, limited by their assumptions to regions where the flow is only weakly dependent on the streamwise coordinate, are not expected to give an adequate description of the motion in the development region near the vessel entrance.

On the other hand, the flow development region may extend over large portions of the aorta, pulmonary artery, and other vessels.[3] Indeed, since many vessels are relatively short, the length required for flow development may be greater than the distance between adjacent branching sites, thus precluding the flows from ever becoming fully developed.

Within the development region, velocity and pressure distributions, and hence the input impedance and vessel wall deformations, can be quite different from those existing in a fully developed flow. Wall shear stresses are usually larger in developing than in fully developed flows. Since endothelial injury has been linked to mechanical stresses imposed by the blood,[4,5] it is possible that flow development plays some role in atherosclerosis; this disease often occurs near vessel junctions. Elastic end effects may also cause localized bending stresses within the vessel walls near their ends.[6]

Some previous analyses have relevance to flow development in the large arteries. Steady flow development in rigid tubes has been investigated extensively[7]; Kuchar and Ostrach[6] extended this work to distensible tubes. Pulsatile flow development in rigid tubes has been studied by Atabek and Chang.[8] However, since both vessel distensibility and unsteadiness can be important in arterial dynamics, it is of interest to investigate flow development including both effects.

II. Mathematical Model

Based on the physical characteristics of the vascular system,[3] a model applicable to the large arteries has been chosen. Blood is assumed to be a homogeneous, incompressible, New-

tonian fluid. The vessel is modelled by a semi-infinitely long, circular, thick-walled, linearly elastic tube, with external tethering stresses to simulate tissue attachments. In addition, it is assumed that the flow is laminar and that the motion of the entire system is axisymmetric and periodic in time.

This model differs from others used in blood flow analyses. It is semi-infinitely long, in contrast to the wave propagation models[1,2] which are infinitely long and thus preclude investigation of development effects. Also, it generalizes the flow development models of Atabek and Chang[8] to the case of a distensible, rather than rigid, tube, and of Kuchar and Ostrach[6] to the case of a pulsatile, rather than steady, flow.

III. Equations and Boundary Conditions

A cylindrical coordinate system R, X, Θ is used, with the origin located on the tube axis in the entrance cross section. At the entrance, the fluid velocity is specified to be axially directed, uniform across the section, and a periodic, nonnegative function of time $F(T)$

$$F(T) = \sum_{n=-N}^{N} F_n e^{in\omega T} \geq 0 \tag{1}$$

Based on the observation that the important harmonic content of typical arterial flows is confined to a small number of the lowest harmonics,[9] the finite Fourier polynomial, Eq. (1), provides a good approximation to a complete Fourier series.

Governing equations for the flow are the continuity and momentum (Navier-Stokes) equations. The important dimensionless parameters of the equations are the mean Reynolds number $Re = aF_0/\nu$ and the unsteadiness parameter $\alpha = a(\omega/\nu)^{1/2}$. Flow in the large arteries is characterized by high Reynolds numbers, typically 10^2 to 10^3, and moderate unsteadiness parameters, usually 10^0 to 10^1. Under these conditions approximations of the boundary-layer kind can be introduced into the equations.[10] That is, the pressure can be considered to be uniform over each cross section and the axial viscous term in the momentum equation can be neglected.

However, the nonlinear convective inertia terms in the momentum equation are not negligible in the development region. Because of mathematical difficulties associated with these terms, a linearization is introduced. This consists of approximating the nonlinear terms $(U\partial U/\partial X + V\partial U/\partial R)$ by $F(T)\,\partial U/\partial X$. Linearizations of this kind have been used previously in analyses of both steady and unsteady flow development,[6-8,11] and agreement with experimental results has been satisfactory.[11,12] Although the technique makes the momentum equation formally linear, a "quasi-nonlinear" behavior remains because both F and U are periodic functions of time. Thus, such nonlinear phenomena as harmonic interactions and harmonic generation are simulated by the linearized equation.

In terms of the dimensionless quantities

$$r = R/a,\ x = X/aRe,\ t = \omega T,\ u = U/F_0$$
$$v = ReV/F_0,\ f = F/F_0,\ p = P/\rho F_0^2 \tag{2}$$

the approximate equations for the flow are

$$\frac{\partial^2 u}{\partial r^2} + \frac{1}{r}\frac{\partial u}{\partial r} - \alpha^2 \frac{\partial u}{\partial t} - f(t)\frac{\partial u}{\partial x} = \frac{\partial p}{\partial x} \tag{3}$$

$$\partial p/\partial r = 0 \tag{4}$$

$$\partial v/\partial r + v/r = -\partial u/\partial x \tag{5}$$

The motion of the tube wall is described by the dynamic equations of elasticity.[13] However, for the physiological ranges of the fluid and tube parameters, and downstream of a small "elastic end effect" region at the entrance (which extends over an initial axial length of the order of the tube radius), these equations can be approximated.[10,14] The axial displacement is small compared to the radial displacement, and axial gradients of the displacements are small compared to radial gradients. Furthermore, wall inertia is unimportant for the frequencies of significance in the arteries. Introducing the dimensionless displacements

$$\eta = H/(\rho F_0^2 a/\mu),\ \xi = \Xi/(\rho F_0 \nu/\mu) \tag{6}$$

the approximate equations for the wall deformation are

$$\partial^2\eta/\partial r^2 + 1/r(\partial\eta/\partial r) - \eta/r^2 = 0 \tag{7}$$

$$\frac{\partial^2 \xi}{\partial r^2} + \frac{1}{r}\frac{\partial \xi}{\partial r} = -(\gamma + 1)\frac{\partial}{\partial x}\left(\frac{\partial \eta}{\partial r} + \frac{\eta}{r}\right) \tag{8}$$

The Lamé coefficient μ and the constant γ are related to the Young's modulus and Poisson ratio by

$$\mu = E/(2 + 2\sigma),\ \gamma = 2\sigma/(1 - 2\sigma) \tag{9}$$

Since the development length is much larger than the tube radius for high Reynolds number flows,[7,8] Eqs. (7) and (8) are valid over all but a very small fraction of the development region. However, solutions of these equations will be used for all $x > 0$.

Turning to the boundary conditions, at the tube entrance the velocity and pressure are specified functions of time,

$$u(0,r,t) = f(t) = \sum_{n=-N}^{N} f_n e^{int} \geq 0 \tag{10a}$$

$$p(0,t) = g(t) = \sum_{n=-N}^{N} g_n e^{int} \tag{10b}$$

At the wall, the fluid and tube velocities are equal. However, since the mean axial fluid velocity is much larger than the axial wall velocity,

$$u(x,1,t) = 0 \tag{11a}$$

provides a good approximation for this component.[10,15] The same approximation cannot be made for the radial components, so that

$$v(x,1,t) = (\rho F_0^2 \alpha^2/\mu)\partial\eta/\partial t(x,1,t) \tag{11b}$$

These conditions are prescribed at the unstressed, rather than the deformed, surface since wall displacements are assumed to be small compared to the unstressed radius. Symmetry conditions along the centerline are

$$\partial u/\partial r(x,0,t) = v(x,0,t) = 0 \tag{12}$$

At the inside and outside tube surfaces the stress vectors within the wall must match those applied by the fluid and surrounding tissues. Downstream of the small "elastic end effect" region, and for the physiological ranges of the fluid and tube parameters, this condition yields, at the inside surface,[14]

$$(\gamma + 2)(\partial\eta/\partial r)(x,1,t) + \gamma\eta(x,1,t) = -p(x,t) \tag{13a}$$

$$\frac{\partial \xi}{\partial r}(x,1,t) + \frac{\partial \eta}{\partial x}(x,1,t) = \frac{\partial u}{\partial r}(x,1,t) \tag{13b}$$

On the outside surface it is assumed the tube is subjected to a constant perivascular pressure and an axial tethering shear stress, as described by Patel and Fry[16]; the stress condition at $r = \beta$ is, therefore,[14]

$$(\gamma + 2)\partial\eta/\partial r(x,\beta,t) + \gamma\eta(x,\beta,t)/\beta = -p_e \tag{14a}$$

$$\frac{\partial \xi}{\partial r}(x,\beta,t) + \frac{\partial \eta}{\partial x}(x,\beta,t) = -\left[m_x \frac{\partial^2}{\partial t^2} + c_x \frac{\partial}{\partial t} + k_x\right]\xi(x,\beta,t) \tag{14b}$$

Thus, the motion is described by five partial differential equations for the fluid velocity components, the wall displacement components, and the pressure. The fluid and wall motions are coupled, through the boundary conditions, because the fluid stresses cause the wall deformation and the fluid and wall velocities must match at the inside surface.

IV. Solution for the Wall Deformation

The wall displacements can be easily found in terms of the fluid pressure and velocity. Integration of Eq. (7) and application of the boundary conditions, Eqs. (13a) and (14a), yield the radial displacement η. Using this solution in Eq. (8), ξ is then found by direct integration and application of the remaining boundary conditions, Eqs. (13b) and (14b). Details of the method and a discussion of the results have been given previously.[14] For present purposes, the solutions of most interest are the radial displacement

$$\eta(x,r,t) = \frac{1}{2(\beta^2-1)}\left[\left(\frac{r}{\gamma+1}+\frac{\beta^2}{r}\right)p(x,t) - \left(\frac{\beta^2 r}{\gamma+1}+\frac{\beta^2}{r}\right)p_e\right] \quad (15)$$

and the hoop and shear stresses in the wall, nondimensionalized with (ρF_0^2) and $(\rho\nu F_0/a)$, respectively,

$$\tau_{\theta\theta}(x,r,t) = \frac{1}{(\beta^2-1)}\left[\left(1+\frac{\beta^2}{r^2}\right)p(x,t) - \left(\beta^2+\frac{\beta^2}{r^2}\right)p_e\right] \quad (16)$$

$$\tau_{rx}(x,r,t) = \left[\frac{\partial u}{\partial r}(x,1,t)\frac{1}{r} - \frac{\gamma}{2(\gamma+1)(\beta^2-1)}\frac{\partial p}{\partial x}(x,t)\left(r-\frac{1}{r}\right)\right] \quad (17)$$

One important aspect of these intermediate solutions is that the boundary condition which matches the fluid and tube velocities at the wall, Eq. (11b), can now be rewritten in terms of flow variables alone. Using Eq. (15), Eq. (11b) becomes

$$v(x,1,t) = \epsilon(\partial p/\partial t)(x,t) \quad (18)$$

where ϵ, given by

$$\epsilon = \frac{\rho F_0^2\alpha^2}{2\mu(\beta^2-1)}\left[\beta^2+\frac{1}{\gamma+1}\right] \quad (19)$$

is called the elasticity parameter.

V. Solution for the Flowfield

For motions periodic in time, all dependent variables could be expanded in uniformly convergent Fourier series. However, because of the limited harmonic content of typical arterial flows,[9] the finite Fourier polynomial

$$y(x,r,t) = \sum_{n=-N}^{N} y_n(x,r)e^{int} \quad (20)$$

is a good approximation to a complete Fourier series. Although the limit N is the same as that used in boundary conditions, Eq. (10), generation within the flow of harmonics not present at $x = 0$ can be investigated by setting some of the coefficients in Eq. (10) equal to zero.

In the Fourier plane the flow problem, Eqs. (3, 5, 10, 11a, 12 and 18), becomes

$$\left(\frac{\partial^2}{\partial r^2}+\frac{1}{r}\frac{\partial}{\partial r}-in\alpha^2\right)u_n - \sum_{j=-N}^{N} f_j\frac{\partial u_{n-j}}{\partial x} = \frac{dh_n}{dx} \quad (21)$$

$$(1/r)\partial/\partial r(rv_n) = -\partial u_n/\partial x \quad (22)$$

with boundary conditions

$$u_n(0,r) = f_n,\ h_n(0) = 0 \quad (23)$$

$$u_n(x,1) = 0 \quad (24a)$$

$$v_n(x,1) = in\epsilon[h_n(x)+g_n] \quad (24b)$$

$$\partial u_n/\partial r(x,0) = v_n(x,0) = 0 \quad (25)$$

Here h_n represents the pressure difference $(p_n - g_n)$. In Eq. (21), the effect of the convective inertia term is to produce harmonic interactions, that is, each harmonic is coupled to a number of others. Thus, the u_n must be determined simultaneously, rather than individually.

A useful result derived from Eqs. (22, 24b, and 25) is

$$\frac{\partial}{\partial x}\int_0^1 ru_n dr = -in\epsilon[h_n(x)+g_n] \quad (26)$$

That is, in elastic tubes, $\epsilon \neq 0$, the instantaneous axial flux need not be the same for each cross section.

Since n ranges from $-N$ to N, Eq. (21) represents a set of $(2N+1)$ coupled partial differential equations, while Eq. (26) gives an additional relationship between each u_n and h_n. If Eqs. (21) and (26) can be solved together for the u_n and h_n, the radial component v_n can be found subsequently from Eq. (22).

The variable x can be eliminated from the problem for u_n and h_n by applying the Laplace transformation,

$$\bar{y}(s) = \int_0^\infty y(x)e^{-sx}dx \quad (27)$$

where s is the Laplace parameter. In the Laplace plane, the equations become

$$\left(\frac{d^2}{dr^2}+\frac{1}{r}\frac{d}{dr}-in\alpha^2\right)\bar{u}_n - \sum_{j=-N}^{N} f_j s\bar{u}_{n-j} = s\bar{h}_n - \sum_{j=-N}^{N} f_j f_{n-j} \quad (28)$$

$$\bar{h}_n = \frac{i}{n\epsilon}\left(s\int_0^1 r\bar{u}_n dr - \frac{f_n}{2}\right) - \frac{g_n}{s} \quad (29)$$

with boundary conditions

$$\bar{u}_n(1) = d\bar{u}_n/dr(0) = 0 \quad (30)$$

Equation (28) represents a set of $(2N+1)$ coupled, nonhomogeneous, ordinary differential equations, with Eq. (29) providing another set of $(2N+1)$ relationships between $\bar{u}_n$ and $\bar{h}_n$. It should be noted that $\bar{h}_n$ depends only on parameters, including s.

In matrix notation, Eq. (28) is

$$(D - [A])[\bar{u}] = s[\bar{h}] - [q][f] \quad (31)$$

where $[\bar{u}]$, $[\bar{h}]$, and $[f]$ are column matrices,

$$D = d^2/dr^2 + (1/r)d/dr \quad (32a)$$

is a linear differential operator, and

$$[q] = \begin{bmatrix} 1 & f_1 & \cdots & f_N & & & 0 \\ f_{-1} & 1 & & & & & \\ \vdots & & \ddots & & & & \\ f_{-N} & & & & & & f_N \\ & & & & 1 & & \\ & & & & & \ddots & \\ 0 & & & & & & \\ & & & & f_{-N} & \cdots & 1 \end{bmatrix} \quad (32b)$$

$$[n] = \begin{bmatrix} N & & & & & & \\ & \cdot & & & & & \\ & & \cdot & & & & 0 \\ & & & \cdot & & & \\ & & & & 1 & & \\ & & & & & 0 & \\ & & & & & & -1 \\ & & & & & & \cdot \\ & & & & & & \cdot \\ 0 & & & & & & \\ & & & & & & \cdot \\ & & & & & & \cdot \\ & & & & & & -N \end{bmatrix} \tag{32c}$$

and

$$[A] = s[q] + i\alpha^2[n] \tag{32d}$$

are square matrices of order $(2N + 1)$.

The form of D, the symmetry condition, Eq. (30), and the fact that the right side of Eq. (31) is independent of r suggest a solution of the form $[\bar{u}] = I_0(\lambda^{1/2}r)\,[e] + [a]$, where λ is a constant scalar and $[e]$ and $[a]$ are constant, nonzero, column matrices. Substitution yields

$$(\lambda[I] - [A])[e] = 0 \tag{33a}$$

and

$$[a] = [A]^{-1}([q][f] - s[\bar{h}]) \tag{33b}$$

Equation (33a) is an eigenvalue problem; that is, $[e]$ is the eigenvector of $[A]$ associated with the eigenvalue λ. There exist $(2N + 1)$ eigenvalues, λ_n, given by the roots of

$$\det([A] - \lambda[I]) = 0 \tag{34}$$

and hence there are $(2N + 1)$ eigenvectors, $[e_n]$. The general solution is a linear combination of the normal modes

$$[\bar{u}] = [m][c] + [a] \tag{35a}$$

where $[m]$ is a square matrix having the normal modes, $I_0(\lambda_n^{1/2}r)\,[e_n]$, as columns and $[c]$ is column matrix of constants. The boundary condition at $r = 1$, Eq. (30), yields $[c] = -[m_1]^{-1}[a]$, where $[m_1]$ is $[m]$ evaluated at $r = 1$. Thus,

$$[\bar{u}] = ([I] - [m][m_1]^{-1})[a] \tag{35b}$$

Using this result in Eq. (29), the matrix $[\bar{h}]$ is

$$[\bar{h}] = [\epsilon[n] + is^2(\tfrac{1}{2}[I] - [m_2][m_1]^{-1})[A]^{-1}]^{-1} \times [is(\tfrac{1}{2}[I] - [m_2][m_1]^{-1})[A]^{-1}[q][f] - \frac{i}{2}[f] - \frac{\epsilon}{s}[n][g] \tag{36}$$

where $[m_2]$ is a square matrix having $\lambda_n^{-1/2}I_1(\lambda_n^{1/2})\,[e_n]$ as columns. Thus $[\bar{h}]$ can be eliminated from $[a]$, leaving $[\bar{u}]$ as an explicit function of r and the parameters.

It remains to invert the solutions back to the Fourier plane by use of the Laplace inversion theorem

$$y(x) = \frac{1}{2\pi i}\int_{C-i\infty}^{C+i\infty} \bar{y}(s)e^{sx}ds \tag{37}$$

The functions $\bar{u}_n$ and $\bar{h}_n$ are generally single-valued functions of s, possessing an enumerable infinity of poles, which tend to zero as s approaches infinity or can be made to do so by dividing them by s. In this case the line integral can be replaced by a closed contour, and by Cauchy's theorem the inversion is the sum of the residues of the integrand of Eq. (37) at its poles. Evaluation of the residues is performed by expansion of the integrand in power (Laurent) series about each pole.

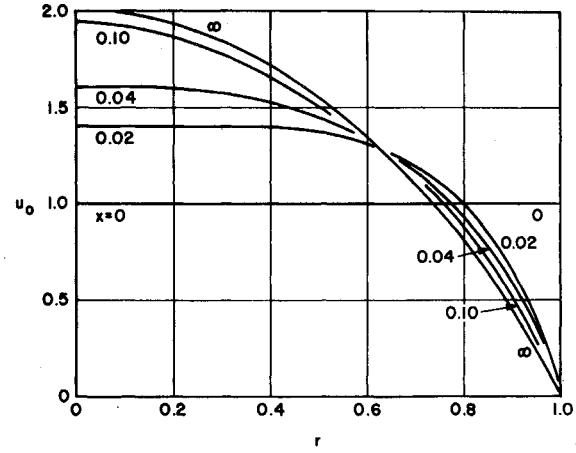

Fig. 1 Velocity of the steady component in the development region.

VI. Case $N = 1$

An example which illustrates the behavior of pulsatile flow development, the influence of the parameters, and harmonic interactions is the case when $N = 1$ and $f_1^2 \ll 1$. The entrance velocity thus consists of small oscillation of a single frequency superimposed on a steady component; generation of higher harmonics is not considered. The effect of neglecting squares of oscillatory components compared to unity is to simplify the matrix $[q]$ to

$$[q] = \begin{bmatrix} 1 & f_1 & 0 \\ 0 & 1 & 0 \\ 0 & f_{-1} & 1 \end{bmatrix} \tag{38}$$

Thus, the influence of the oscillatory component on the development of the steady flow is negligible, but the steady component has a unit order effect on the development of the oscillatory flow.

Following the method of solution discussed above, the velocity solutions in the Fourier plane are

$$u_0 = 2(1 - r^2) - \sum_{j=1}^{\infty} \frac{4}{\beta_j}\left[1 - \frac{J_0(\beta_j^{1/2}r)}{J_0(\beta_j^{1/2})}\right]e^{-\beta_j x} \tag{39a}$$

$$u_1 = \frac{4if_1}{\alpha^2}\sum_{j=1}^{\infty}\left\{\left[1 - \frac{J_0(\beta_j^{1/2}r)}{J_0(\beta_j^{1/2})}\right] + K_j\left[1 - \frac{J_0(\gamma_j^{1/2}r)}{J_0(\gamma_j^{1/2})}\right]\right\} \times e^{-\beta_j x} - \frac{4if_1}{\alpha^2}\sum_{j=0}^{\infty} L_j\left[1 - \frac{J_0(\delta_j^{1/2}r)}{J_0(\delta_j^{1/2})}\right]e^{-\kappa_j x} \tag{39b}$$

The solution for u_{-1} is just the conjugate of u_1. In these

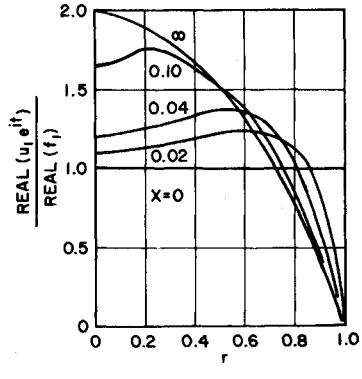

Fig. 2 Velocity of the oscillatory component in the development region for $\alpha = 1$, $t = 0$, and f varying as cost.

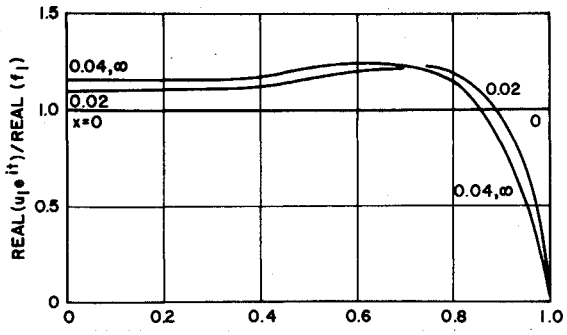

Fig. 3 Velocity of the oscillatory component in the development region, for $\alpha = 10$, $t = 0$, and f varying as cost.

solutions,

$$K_j = \frac{2\epsilon\beta_j J_0(\gamma_j^{1/2})}{2\epsilon\gamma_j J_0(\gamma_j^{1/2}) + i\beta_j^2 J_2(\gamma_j^{1/2})} \tag{40a}$$

$$L_j = \left\{\kappa_j^3\delta_j + 2\epsilon\kappa_j^2\left[\alpha^2\left(2 + \frac{g_1}{f_1}\right) - i\kappa_j\frac{J_0(\kappa_j^{1/2})}{J_2(\kappa_j^{1/2})}\right]\right\}\Big/ \kappa_j^4 + 4\epsilon\kappa_j(4\alpha^2 + i\delta_j\kappa_j) - 4\epsilon^2\delta_j^2 \tag{40b}$$

$$\gamma_j = \beta_j - i\alpha^2 \tag{40c}$$

and

$$\delta_j = \kappa_j - i\alpha^2 \tag{40d}$$

The quantities β_j and κ_j are the roots of the characteristic equations

$$J_2(\beta_j^{1/2}) = 0 \qquad (\beta_j \neq 0) \tag{41a}$$

$$\kappa_j^2 J_2(\delta_j^{1/2}) - 2i\epsilon\delta_j J_0(\delta_j^{1/2}) = 0 \qquad (\delta_j = 0) \tag{41b}$$

Solutions of Eq. (41a) are well known, but those of Eq. (41b) are in general complex and must be determined numerically as functions of the two parameters ϵ and α. However, the elasticity parameter ϵ is a small parameter, having values of order 10^{-2} or smaller in the vessels. Thus, it is possible to obtain estimates of the roots and the solutions by a perturbation about $\epsilon = 0$, the rigid tube limit.

In the limit as ϵ approaches zero, the roots of Eq. (41b) are given by

$$\kappa_0 = 0 \tag{42a}$$

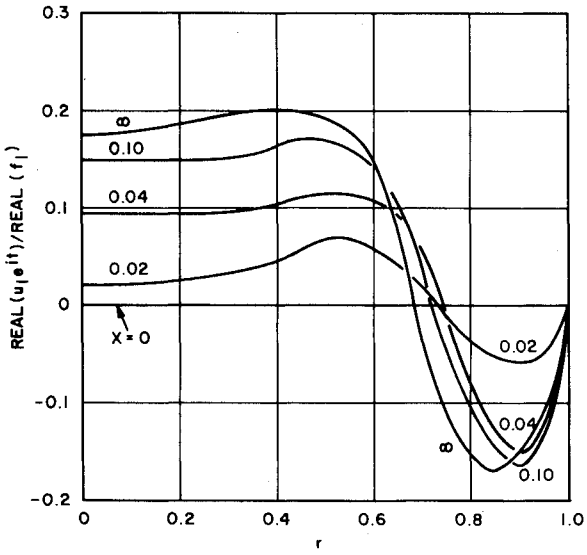

Fig. 4 Velocity of the oscillatory component in the development region, for $\alpha = 10$, $t = \pi/2$ and f varying as cost.

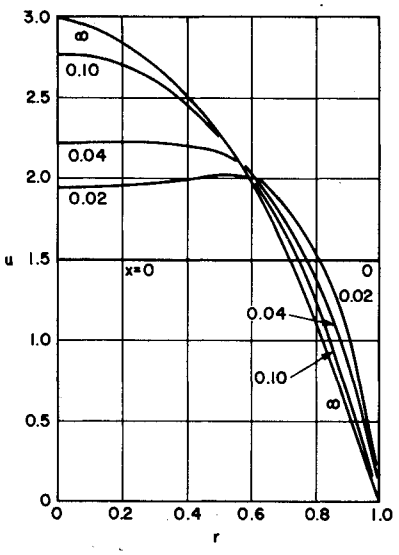

Fig. 5 Composite velocity in the development region, for $\alpha = 1$, $t = 0$, and $f = 1 + 0.5$ cost.

$$J_2[(\kappa_j - i\alpha^2)^{1/2}] = 0 \tag{42b}$$

and the solution for u_1 becomes

$$u_1 = \frac{f_1}{J_2(i^{3/2}\alpha)}\left[J_0(i^{3/2}\alpha r) - J_0(i^{3/2}\alpha)\right] + \frac{4if_1}{\alpha^2}\sum_{j=1}^{\infty} \times \left[1 - \frac{J_0(\beta_j^{1/2}r)}{J_0(\beta_j^{1/2})}\right]\left[1 - \frac{\beta_j}{\beta_j + i\alpha^2}e^{-i\alpha^2 x}\right]e^{-\beta_j x} \tag{43}$$

Higher approximations can be obtained by expanding the roots of Eq. (41b) in powers of $\epsilon^{1/2}$. To order $\epsilon^{1/2}$, the root κ_0 is

$$\kappa_0 = \pm[2\alpha^2 J_0(i^{3/2}\alpha)/J_2(i^{3/2}\alpha)]^{1/2}\epsilon^{1/2} \tag{44}$$

while to this order the roots given by Eq. (42b) are unchanged; these latter roots change only at order ϵ. The solution for u_1 to order $\epsilon^{1/2}$ is given by Eq. (43), except that the first term on the right side is multiplied by $e^{-\kappa_0 x}$, with κ_0 given by Eq. (44).

The influence of ϵ on the solutions in the development region can be investigated by another technique. With arbitrary ϵ, the solutions in the Fourier plane for small x can be found by expanding the solutions in the Laplace plane in asymptotic series for large s, and then inverting term by

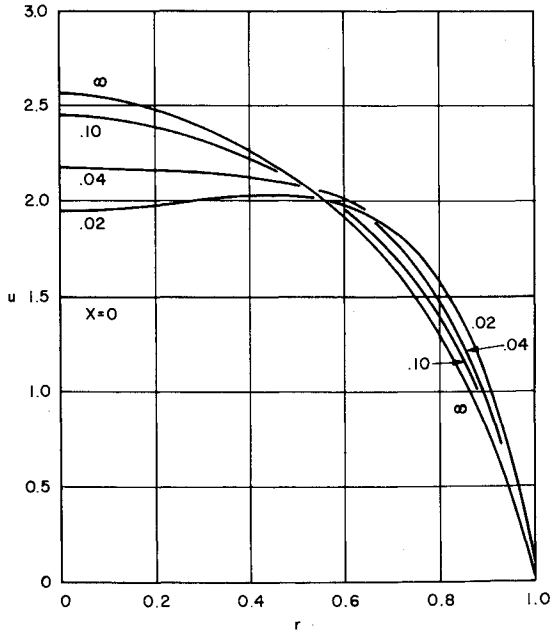

Fig. 6 Composite velocity in the development region for $\alpha = 10$, $t = 0$, and $f = 1 + 0.5$ cost.

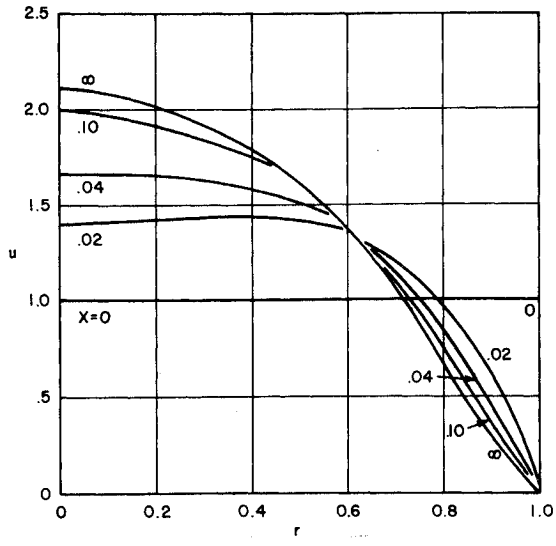

Fig. 7 Composite velocity in the development region for $\alpha = 10$, $t = \pi/2$, and $f = 1 + 0.5 \cos t$.

term.[17] As an example, the result for p_1 is

$$p_1 = g_1 \left\{ 1 - \frac{4f_1}{\Gamma(3/2)} x^{1/2} - \left[(6 + i\alpha^2) \frac{f_1}{g_1} - i\epsilon \right] x + \ldots \right\} \tag{45}$$

Solutions of this type are valid only for small x, but apply for arbitrary ϵ.

VII. Discussion

Some idea of the nature of development effects can be gained by examining the velocity profiles. The velocity consists of the sum of the steady and oscillatory components. Profiles for the individual components, based on Eqs. (39a) and (43), with $\epsilon = 0$, are depicted in Figs. 1–4.

In the steady flow development, Fig. 1, a boundary layer exists near the entrance, but for x larger than about 0.04 the sheared region has reached to the centerline. A parabolic profile is attained asymptotically as x increases.

The profiles for the oscillatory component, Figs. 2–4, differ markedly from those for the steady component. This is due to both the effect of harmonic interaction with the steady component and the fact that the fully developed oscillatory profiles are functions of α and time, which tend to become flattened and exhibit backflow near the wall as α increases above unity.

The extent of the development region in an oscillatory flow depends on time. For example, the profiles in Fig. 3 are independent of x for x larger than 0.04. However, at a different time in the pulse cycle (Fig. 4) the development occurs over a much longer region.

Composite profiles, which add the steady and oscillatory components, are shown in Figs. 5–8 for an entrance velocity

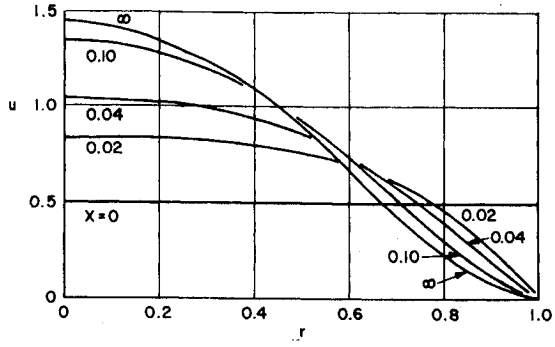

Fig. 8 Composite velocity in the development region for $\alpha = 10$, $t = \pi$, and $f = 1 + 0.5 \cos t$.

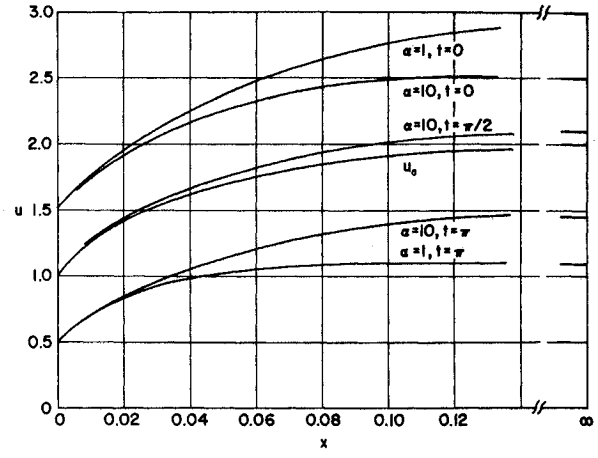

Fig. 9 Axial development of the velocity along the centerline, for $f = 1 + 0.5 \cos t$.

$f = 1 + 0.5 \cos t$, that is, $f_1 = 0.25$. At the time of the greatest forward flow, $t = 0$, the profiles are flatter than those for a steady flow alone. The degree of flatness increases, and hence the maximum velocity reached at the centerline decreases, with increasing α (Figs. 5–6). A sequence of profiles for different times in the pulse cycle, but constant α, are given in Figs. 6–8. The inflection points near the wall at times $t = \pi/2$ and $t = \pi$ are due to flow reversal in the oscillatory component.

The development length can be determined by examining the variation of velocity with x at a given radial position, taken to be the centerline in Fig. 9. A standard criterion is to define the development length to be that x where these curves reach 99% of their asymptotic values. For steady flow, the dimensionless development length is then 0.16. In pulsatile flow the development length depends on α, the f_n, and time. For example, in the case for $\alpha = 1$, the development length at $t = 0$ is 0.24, while at $t = \pi$ it is about 0.08. Thus, the development length oscillates about the steady value, the magnitude of the oscillation being dependent on the f_n and α. This is consistent with the findings of Atabek and Chang.[8]

Based on the observation that the development length in steady flow is proportional to the Reynolds number, that is, proportional to the velocity at the tube entrance, it is of interest to replot Fig. 9 in coordinates based on the instantaneous, rather than steady, velocity. This can be done by dividing both u and x by f, and the results are shown in Fig. 10. Here the curve for $\alpha = 0$ applies for both steady flow and for pulsatile flow in the limit as α approaches zero. The curves for $\alpha = 1$ virtually duplicate that for $\alpha = 0$, so that this curve can be used to determine the development length for pulsatile flows in the range $\alpha \leq 1$. For values of α higher than unity, the curves deviate from that for $\alpha = 0$ and depend on time, indicating that unsteadiness is influencing the flow development to a greater degree.

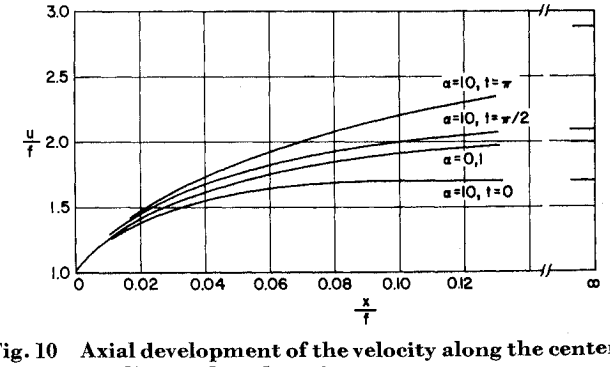

Fig. 10 Axial development of the velocity along the centerline in coordinates based on instantaneous entrance velocity, for $f = 1 + 0.5 \cos t$.

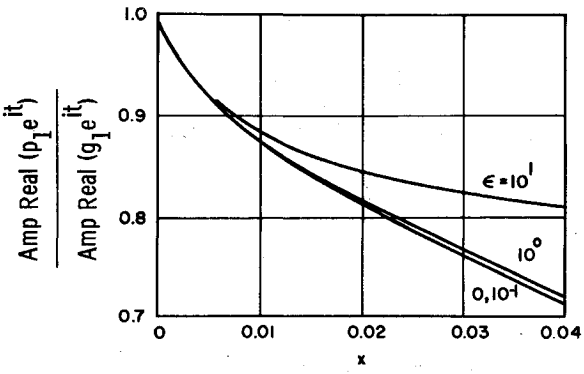

Fig. 11 Effect of the elasticity parameter on the amplitude of the oscillatory component of the pressure.

In the cases investigated, the development lengths ranged from about half to twice the steady flow value of 0.16 aRe. For Reynolds numbers in the arterial range, 10^2 to 10^3, this length is comparable to the total lengths of many vessels, which lie in the range of $80a$ to $150a$. Thus, development effects can occur over large portions of major vessels if the entrance profiles are flat. The effect of entrance profiles which are not axisymmetric or are not flat has not been determined.

For very small values of x the shear stress at the wall, given by Eq. (17), is much higher than that farther downstream. If intimal injury is due to high shear,[4,5] it would appear that that region close to the vessel entrance would be most susceptible to injury.

Thus far the effect of the elasticity parameter has not been discussed. Using Eq. (45), which is valid near $x = 0$ for arbitrary ϵ, the amplitude of the oscillatory component of the pressure is shown for a range of ϵ in Fig. 11. For values of ϵ up to 10^{-1}, there are negligible deviations from the results for a rigid tube, $\epsilon = 0$. At higher values of ϵ elasticity does affect the oscillatory pressure gradient. However, since the elasticity parameter is of order 10^{-2} or smaller in the vascular system, these results indicate that vessel distensibility has little influence on flow development. This conclusion is reinforced by the analysis given in the previous section that indicated that if the first term on the right side of Eq. (43) is multiplied by $e^{-\kappa_0 x}$, with κ_0 given by Eq. (44), then the solution is correct to order $\epsilon^{1/2}$, with neglected effects only of order ϵ.

It is of interest to examine the solutions for u_1 valid to order one and order $\epsilon^{1/2}$. Since the β_j are real, the second term on the right side of Eq. (43) vanishes as x increases, leaving only the first term, which then represents the fully developed oscillatory flow. To order one, that is, the limit of $\epsilon = 0$, the first term is indeed identical to the solution for fully developed flow in a rigid tube found by Womersley[1] and others. To order $\epsilon^{1/2}$, when the first term is multiplied by $e^{-\kappa_0 x + it}$, the fully developed oscillatory flow has a traveling-wave behavior with dimensional complex wave velocity given by

$$c^2 = \frac{\mu(\beta^2 - 1)(1 + \gamma)}{\rho[\beta^2(\gamma + 1) + 1]}\left[1 - \frac{2J_1(i^{3/2}\alpha)}{i^{3/2}\alpha J_0(i^{3/2}\alpha)}\right] \quad (46)$$

This is just the fully developed solution for wave propagation and oscillatory flow in thick-walled elastic tubes.[2,14] Thus, the solutions found here apply to both the development and fully developed regions and give a unified theory for blood flow in arteries.

VIII. Conclusions

A mathematical model for investigating flow development in the large arteries has been presented. It includes the effects of viscosity, pulsatile flow, and vessel elasticity. Velocity profiles, pressure distributions, wall displacements, and wall stresses were found analytically for the high Reynolds number regime.

For the physiological ranges of the flow and wall parameters, it was found that the developing flow has a strong boundary-layer character, resulting in high wall shear stresses near the vessel entrances, a phenomenon of interest for intimal injury. The development length depends primarily on the mean Reynolds number, the unsteadiness parameter, and the amplitude of oscillatory flow at the tube entrance; for typical cases this length is quite large, indicating that development effects can exist over much of the aorta and other major vessels. Effects of wall distensibility on flow development are not significant for physiologically normal distensibilities.

Within the development region, harmonic interactions and harmonic generation occur. As the distance from the entrance increases, however, the solutions found approach the fully developed, traveling-wave type considered in most previous analyses of blood flow. The present analysis thus gives a total description of blood flow from the vessel entrance through the fully developed region.

In conclusion, flow development effects can be significant in the large arteries, and a knowledge of their characteristics is necessary for an understanding of vascular dynamics.

References

[1] Womersley, J. R., "An Elastic Tube Theory of Pulse Transmission and Oscillatory Flow in Mammalian Arteries," TR 56-614, 1957, Wright Air Development Center, Ohio.

[2] Cox, R. H., "Comparison of Linearized Wave Propagation Models for Arterial Blood Flow Analysis," *Journal of Biomechanics*, Vol. 2, 1969, pp. 251–265.

[3] McDonald, D. A., *Blood Flow in Arteries*, Edward Arnold, London, 1960.

[4] Texon, M., "The Role of Fluid Mechanics in the Development of Atherosclerosis," *Proceedings of the Annual Conference on Engineering in Medicine and Biology*, Vol. 10, 1968, p. 49B.2.

[5] Fry, D. L., "Acute Vascular Endothelial Changes Associated with Increased Blood Velocity Gradients," *Circulation Research*, Vol. 22, 1968, pp. 167–197.

[6] Kuchar, N. R. and Ostrach, S., "Flows in the Entrance Regions of Circular Elastic Tubes," *Biomedical Fluid Mechanics Symposium*, 1966, American Society of Mechanical Engineers, pp. 45–69.

[7] Lew, H. S. and Fung, Y. C., "Entry Flow into Blood Vessels at Arbitrary Reynolds Number," *Journal of Biomechanics*, Vol. 3, 1970, pp. 23–38.

[8] Atabek, H. B. and Chang, C. C., "Oscillatory Flow near the Entry of a Circular Tube," *Zeitschrift für Angewandte Mathematik und Physik*, Vol. 12, 1961, pp. 185–201.

[9] Attinger, E. O., Anné, A., and McDonald, D. A., "Use of Fourier Series for the Analysis of Biological Systems," *Biophysical Journal*, Vol. 6, 1966, pp. 291–304.

[10] Kuchar, N. R., "Unsteady Entrance Flows in Circular Elastic Tubes with Application to the Vascular System," Ph.D. thesis, 1967, Case Western Reserve University, Cleveland, Ohio.

[11] Sparrow, E. M., Lin, S. H., and Lundgren, T. S., "Flow Development in the Hydrodynamic Entrance Regions of Tubes and Ducts," *The Physics of Fluids*, Vol. 7, 1964, pp. 338–347.

[12] Florio, P. J. and Mueller, W. K., "Development of a Periodic Flow in a Rigid Tube," *Transactions of the ASME: Ser. D*, Vol. 90, 1968, pp. 395–399.

[13] Sokolnikoff, I. S., *Mathematical Theory of Elasticity*, McGraw-Hill, New York, 1956, p. 80.

[14] Kuchar, N. R. and Ostrach, S., "A Thick-Walled Viscoelastic Model for the Mechanics of Arteries," *Journal of Biomechanics*, Vol. 2, 1969, pp. 443–454.

[15] Patel, D. J., Mallos, A. J., and Fry, D. L., "Aortic Mechanics in the Living Dog," *Journal of Applied Physiology*, Vol. 16, 1961, pp. 293–299.

[16] Patel, D. J. and Fry, D. L., "Longitudinal Tethering of Arteries in Dogs," *Circulation Research*, Vol. 19, 1966, pp. 1011–1021.

[17] Carslaw, H. S. and Jaeger, J. C., *Operational Methods in Applied Mathematics*, Dover, New York, 1963.